

# Final activities report

Vladimir Pietro Cravero

Fermi National Accelerator Laboratory  
Batavia, IL

July 30, 2012 - September 28, 2012

# Contents

<b>1</b>	<b>Taper machine</b>	<b>2</b>
1.1	introduction . . . . .	2
1.2	Schematic . . . . .	2
1.3	Programming . . . . .	2
1.4	Conclusions . . . . .	3
<b>2</b>	<b>AC dipole</b>	<b>4</b>
2.1	Introduction . . . . .	4
2.1.1	Magnet model . . . . .	4
2.2	Power measurement . . . . .	5
2.2.1	Experimental setup . . . . .	5
2.2.2	5.1MHz power measurement . . . . .	5
2.2.3	300kHz power measurement . . . . .	7
2.2.4	Cable delay . . . . .	8
2.2.5	Conclusions . . . . .	10
2.3	Multimodal excitation . . . . .	11
2.3.1	Introduction . . . . .	11
2.3.2	Filter . . . . .	11
2.3.2.1	Schematic . . . . .	11
2.3.2.2	Transfer function . . . . .	11
2.3.2.3	AC response . . . . .	12
2.3.2.4	Impedance . . . . .	13
2.3.3	Modified filter . . . . .	14
2.3.3.1	Schematic . . . . .	14
2.3.4	First prototype . . . . .	15
2.3.4.1	Construction . . . . .	15
2.3.4.2	Testing . . . . .	16
2.3.5	Further development . . . . .	18
2.3.5.1	Go for higher power . . . . .	18
2.3.5.2	Automated wave tuning . . . . .	18
2.3.6	Conclusions . . . . .	18
<b>3</b>	<b>Ringer</b>	<b>19</b>
3.1	Introduction . . . . .	19
3.2	Theoretical treatise and setup . . . . .	19
3.3	Conclusions . . . . .	20

# Chapter 1

## Taper machine

### 1.1 introduction

The taper machine will be used to insulate superconducting wire employed in the CLAS12 magnet coils. A totally new design was necessary because the particular kind of cable used in this magnet is slightly wider than the kind of cable normally employed. It was decided to use a servomotor with a PLC and an optical encoder due to their precision, the expansion possibilities and the HMI support for safe and easy machine controlling.

### 1.2 Schematic

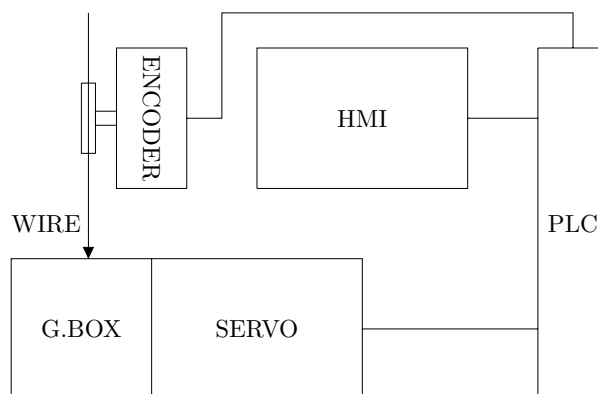


Figure 1.1: Schematic

The wire that needs to be wrapped is fed to the machine passing on a rubber wheel attached to the encoder and through a gearbox. The insulator spool will be connected to the gearbox output shaft that will be controlled by the PLC according to the encoder input in order to ensure proper wrapping. The HMI will allow the operator to set various parameters such as wrapping pitch and coverage, and to measure the wire and insulator used.

### 1.3 Programming

The PLC programming was done in Visual Basic, while the HMI was personalized using dedicated Baldor software.

The implemented characteristics are:

- Start, stop, enable and jog controls connected directly to the servomotor controller
- Status led indicators connected directly to the servomotor controller
- To-be-wrapped wire speed and length measurement
- Used up insulating tape length measurement
- Running out wire or insulator alarms with adjustable thresholds
- Wrapping pitch and coverage fine tune
- Jogging speed real time regulation
- Remote HMI constituted by a LCD screen and a small keyboard to display and insert data

Safety was a concern too: the firmware is written so that emergency events as stop button pressing or motor overload are processed as soon as possible, braking the motor and disabling it.

## 1.4 Conclusions

The software was not fully tested because of the absence of the hardware to build the full machine and will need further trimming when it will be built. Its modular nature will allow easy and deep field testing, as well as easy bug tracking and correction.

# Chapter 2

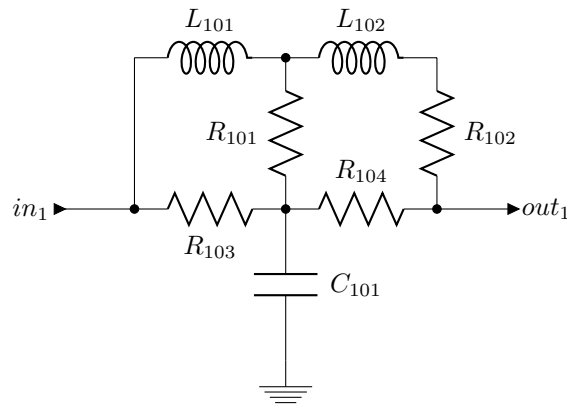
## AC dipole

### 2.1 Introduction

The AC dipole I worked on is a magnet that will be used in the  $\mu 2e$  experiment to deflect periodically the muon beam in order to reduce the noise picked up by the detector. The final setup should consist of a row of magnets excited at different frequencies and powers, so measuring the power was important to verify if the prototype could meet the specifications. Some experiments on multimodal excitation were performed too, that is feeding the same magnet with both the frequencies needed through an analog bi resonant filter.

#### 2.1.1 Magnet model

A magnet model has been made utilizing the same cell repeated 24 times. The cells are connected in two series of twelve, and the two series can be connected in series externally. The base cell schematic follows.



Where:

- $R_{101} = R_{102} = 100 \mu\Omega$
- $R_{103} = R_{104} = 50 \Omega$
- $L_{101} = L_{102} = 200 \text{ nH}$
- $C_{101} = 36.5 \text{ pF}$

As said, each input node is connected to the previous stage output node so that the accessible nodes are  $in_1, out_{12}, in_{13}$  and  $out_{24}$ . The nodes  $out_{12}$  and  $in_{13}$  usually are interconnected to a capacitor dimensioned for the desired resonant frequency.

## 2.2 Power measurement

### 2.2.1 Experimental setup

The excitement circuits for both frequencies are quite similar, so the measuring setup and hardware were similar too. Current and voltage measurements were performed using a current probe and two voltage probes in differential mode, both on the primary and on the secondary of the coupling transformer. The data was collected with a LeCroy scope, and both print of the waveforms and raw data point dump were saved and later used to calculate the power.

In the 5.1MHz excitation circuit a signal generator provided a sine wave that was fed to a RF amplifier. The amplified signal passed through a coupling transformer and a bank of decoupling capacitors, then was fed in the magnet. The resonant frequency could be matched varying the sinusoid frequency.

In the 300kHz configuration instead the magnet was connected to two capacitors bank in order to let it resonate at 300kHz. A 300kHz square wave was fed to it through a coupling transformer, and its frequency could be trimmed to pinpoint the resonant frequency.

### 2.2.2 5.1MHz power measurement

The 5.1MHz waves follow, both for primary and secondary:

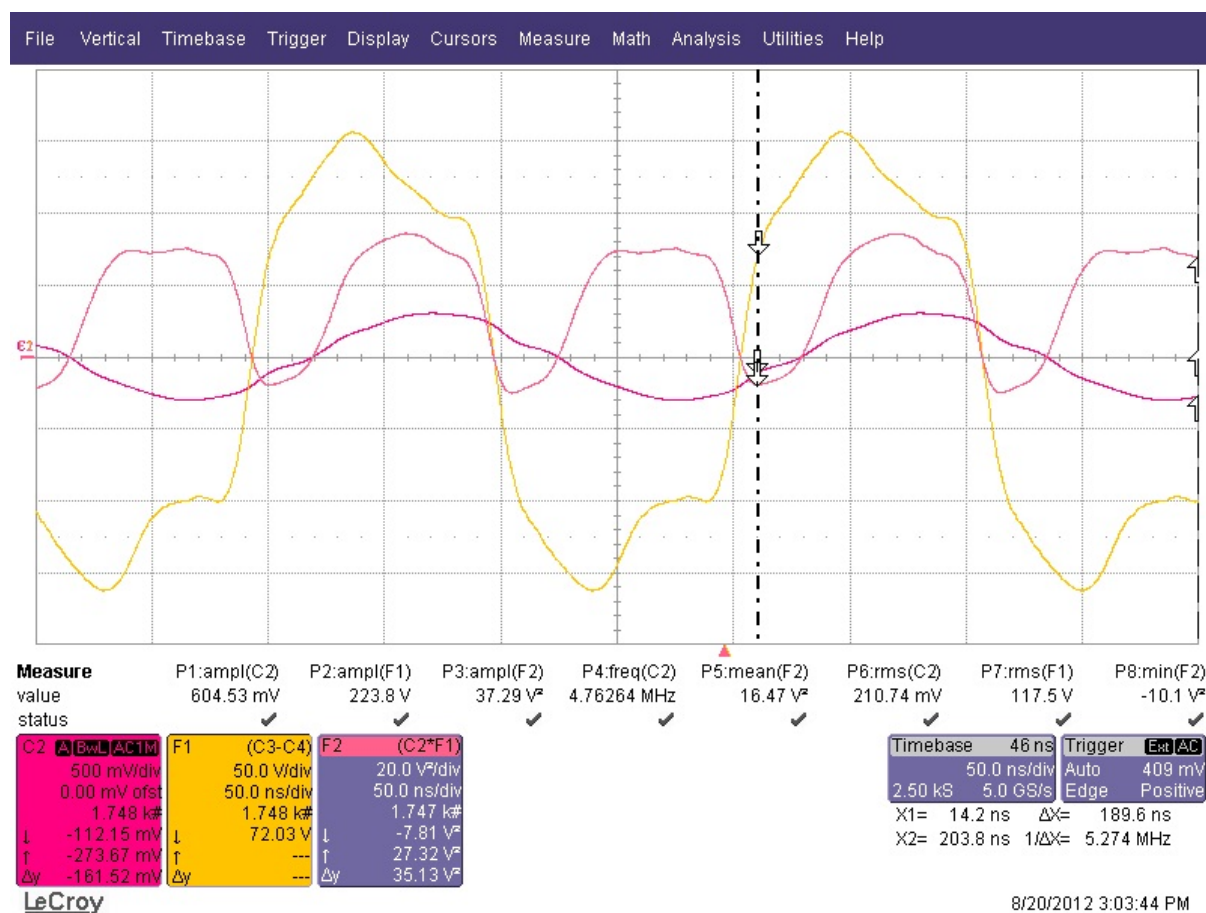


Figure 2.1: Primary

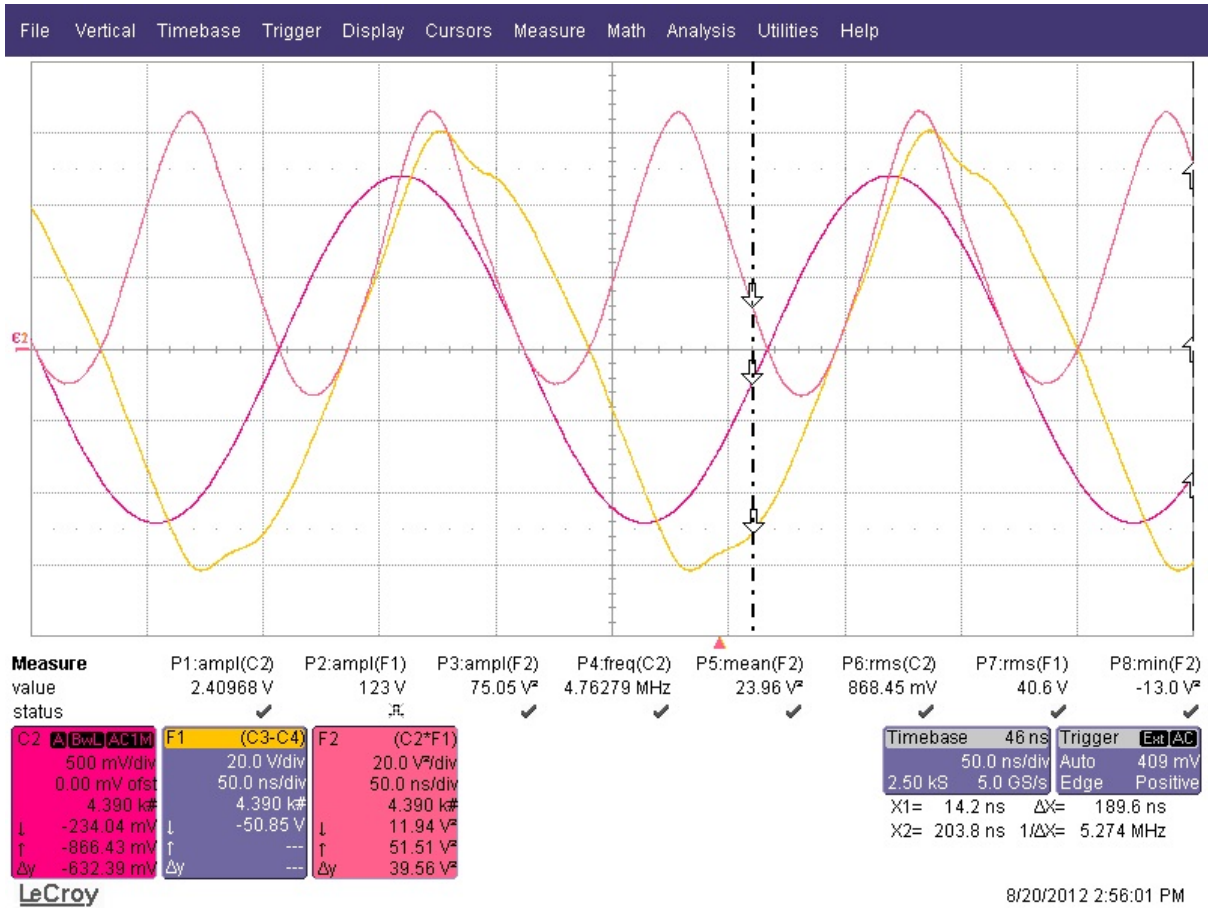


Figure 2.2: Secondary

Where:

- C2 is the current,  $5 \frac{A}{div}$
- F1 is the voltage, 50 or  $20 \frac{V}{div}$  respectively
- F2 is the instantaneous power,  $200 \frac{W}{div}$

The average power was computed integrating the power signal over one voltage period and dividing by the period duration. The values obtained for the primary and the secondary are:

$$P_{avg,pri} = 162W \quad P_{avg,sec} = 243W$$

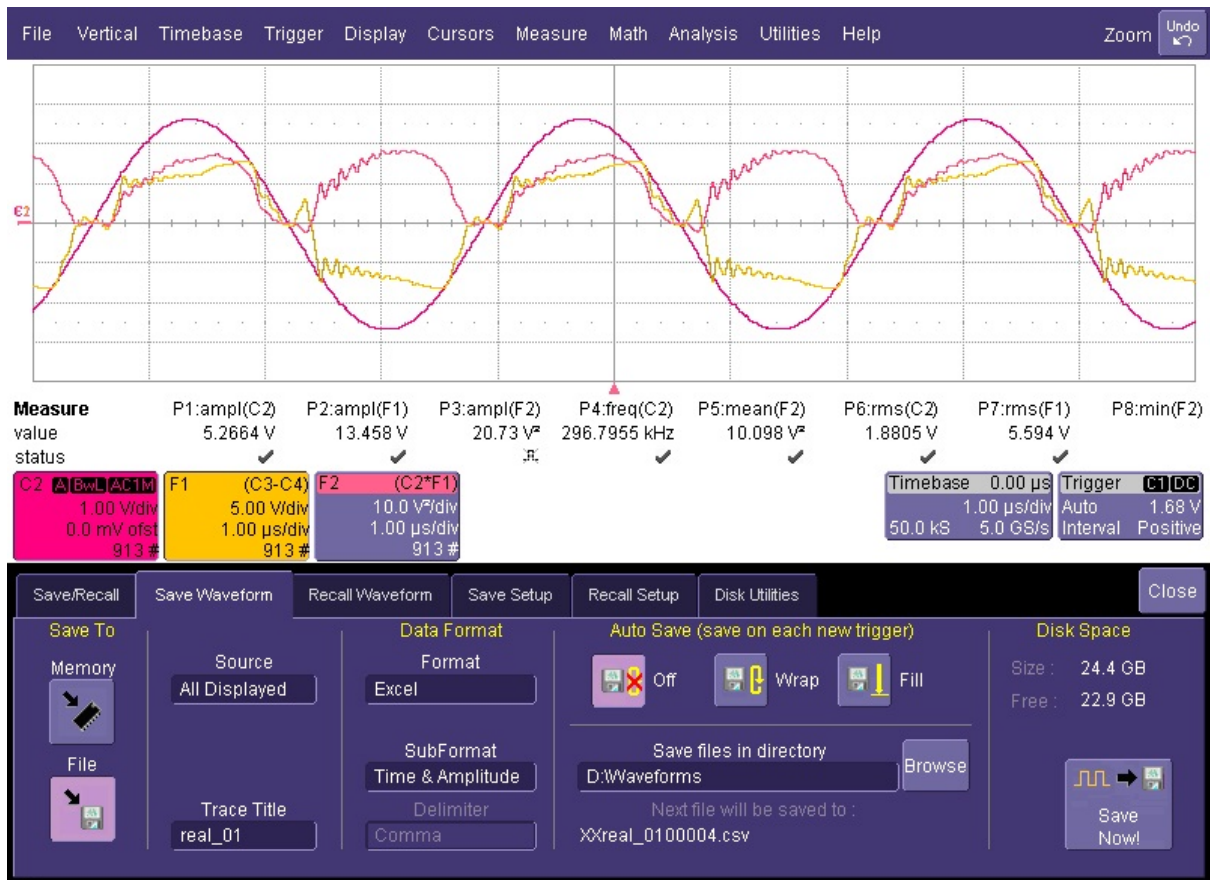
These numbers are clearly wrong, but applying the measured cable delay, that is 9ns, the values are:

$$P_{avg,pri} = 201W \quad P_{avg,sec} = 166W$$

that are much more reliable.

### 2.2.3 300kHz power measurement

The 300kHz waves follow, again both for primary and secondary:



F2 has been saved in D:\Waveforms\F2real\_0100003.csv

Figure 2.3: Primary

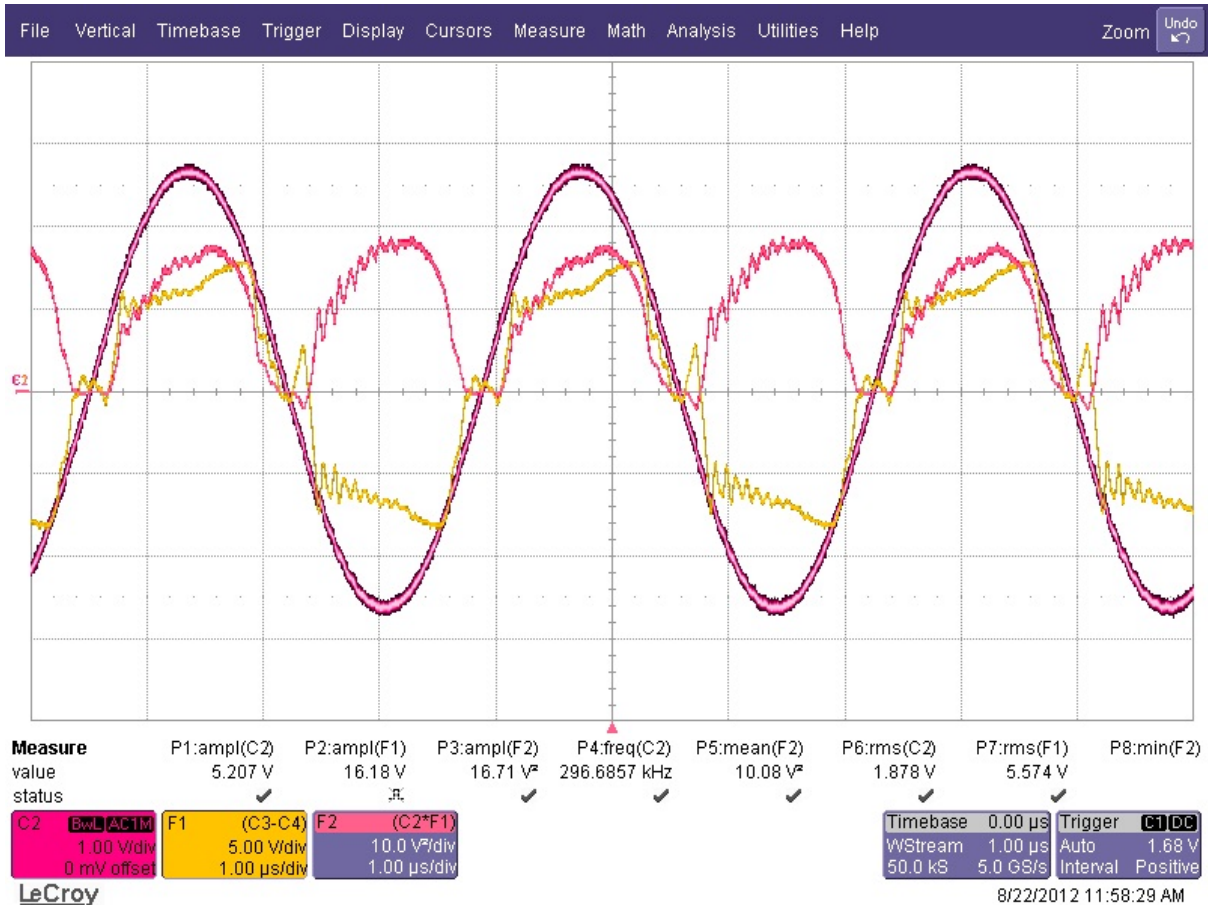


Figure 2.4: Secondary

Where:

- C2 is the current,  $10 \frac{A}{div}$
- F1 is the voltage,  $50 \frac{V}{div}$
- F2 is the instantaneous power,  $1 \frac{kW}{div}$

The average power was computed in the same way as 5.1MHz. The values obtained for the primary and the secondary are:

$$P_{avg,pri} = 1015W \quad P_{avg,sec} = 874W$$

These numbers are quite good because at a slower frequency the few ns delay can be neglected.

## 2.2.4 Cable delay

The fact that the power values measured were wrong was evident when the active power measured on the secondary of a transformer exceeded the power on the primary of a hundred of W. Having both the current and voltage waveforms saved allowed a shifted phase calculation of the power both on the primary and on the secondary. A delay of the current on the primary produced an increase in power, while it decreased it on the secondary. The two power balanced between 6 and 7ns, so a differential delay between the voltage probes and the current loop of about 7ns was foreseen, counting in the transformer efficiency too. The following table contains the values of the average power both on the primary and secondary windings as a function of voltage delay:

Delay (ns)	-2	-1	0	1	2	3	4	5	6	7
$P_{avg,pri}(W)$	151.7	157.2	162.4	167.5	172.4	177.1	181.6	185.9	190.0	193.9
$P_{avg,sec}(W)$	257.6	250.3	242.8	235.0	227.1	219.0	210.6	202.1	193.4	184.5

The hardware used in the experiment follows:

- Digital four channel oscilloscope
- Impulse generator
- High-delay cable
- T-shaped signal splitter
- Current measuring device with 19 windings of stranded wire
- A pair of 3ns matched coaxial cables

The impulse generator was connected to the T splitter through the high delay cable in order to retard the first reflection as much as possible. The T splitter was connected to the oscilloscope through a 3ns cable and to the stranded wire wound around the current measuring device. The oscilloscope input was set at 50Ω to match the impulse generator output impedance thus reducing reflections. The current measuring device was finally connected to another oscilloscope input through the other 3ns cable, and the input was set on high impedance, i.e. 1MΩ. The impulse generator was regulated in order to produce 6V high, 1μs wide pulses at 10kHz, and the rise time measured was about 1ns. The oscilloscope was set at fastest sampling speed, and special care was used to set the trigger to avoid multiple triggering due to reflection.

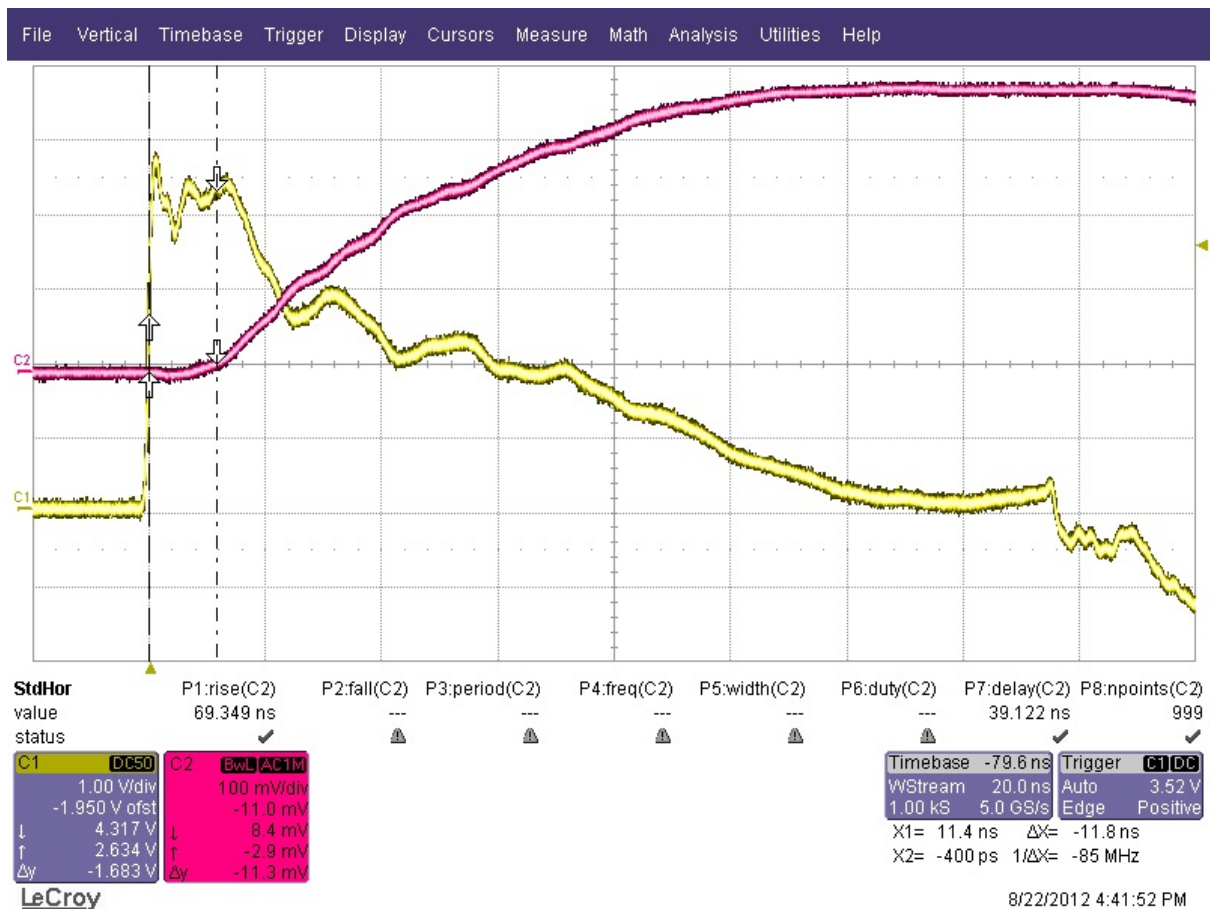


Figure 2.5: Pulse response

The yellow trace represents the impulse generator output, while the fuchsia trace represents the current measured by the device under test. The cursors used to measure the delay can clearly be seen, and on bottom right the delay is reported as  $\Delta X = 11.8\text{ns}$ . This value does not agree with the theoretical calculated value, but there is another delay that must be taken in account: the cables used during power measurement. The voltage probes cables are a little longer than the cable used to connect the current measuring device to the oscilloscope. Assuming that the different cables insulator has the same  $\epsilon_r$ , i.e. the delay time per unit length is the same, measuring the cables length with a tape is enough to compute the additional delay. The cable used during power measurement is about 160cm long and has 8ns delay, so the delay time per unit length is about 5ns/m. The voltage probe cables are about 60cm longer than the 8ns cable, resulting in a differential delay of about 3ns.

Summing up, the current measuring device introduces a delay of about 12ns, while the voltage probe cables are 3ns slower than the cable used for the current probe, resulting in a total of 9ns delay for the current.

The foreseen and measured delays differ for about the 20% mainly because the delay between the impulse and the current probe answer is not clear because the two waveforms are quite different. Moreover, moving the cursors as little as  $\frac{1}{20}$  of division results in a variation of the measured delay of 1ns.

### 2.2.5 Conclusions

The power measurement performed were reassuring: the specifications were met with a good margin both for 5.1MHz and 300kHz. The measurement difficulties were overcome, and reliable data was obtained.

## 2.3 Multimodal excitation

### 2.3.1 Introduction

The most difficult part of this part of the project was the filter design. The literature about double bandpass filters is lacking and concerns stripline microwave filters only, which are low-power, high frequency solutions not suitable for our application.

The only practical constraint was the use of passive components to be able to scale the circuit up to the desired power, and the possibility to regulate the turn off time varying inductance values so that an automated wave tuning controller could be built using linear actuators that move the ferrite core of the coils.

A series-parallel partitive LC filter was finally chosen because it satisfied all the requirements. Moreover, a preliminary Laplace domain study showed that its frequency response fitted perfectly our needs.

### 2.3.2 Filter

#### 2.3.2.1 Schematic

The basic electrical scheme of the filter follows:

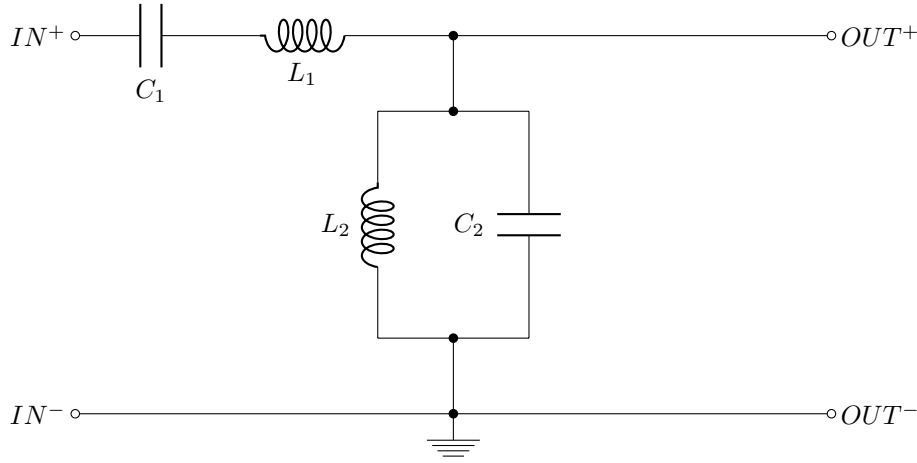


Figure 2.6: Ideal filter

#### 2.3.2.2 Transfer function

The output voltage is a partition of the input voltage, a simple calculation in the s-domain will eventually lead to:

$$\frac{V_{out}}{V_{in}} = \frac{L_2 C_1 s^2}{L_1 C_1 L_2 C_2 s^4 + (L_2 C_1 + L_1 C_1 + L_2 C_2) s^2 + 1} \quad (2.1)$$

The transfer function has two zeros in the origin and four poles. The poles can be proven to be complex looking at the quadratic equation:

$$L_1 C_1 L_2 C_2 t^2 + (L_2 C_1 + L_1 C_1 + L_2 C_2) t + 1 = 0 \quad (2.2)$$

If  $t_1$  and  $t_2$  are solutions of (2.2), the four poles will be  $s_{1,2} = \pm\sqrt{t_1}$  and  $s_{3,4} = \pm\sqrt{t_2}$ , but  $t_1, t_2 < 0$  because if  $p = t_1 t_2$  and  $s = t_1 + t_2$  we can write:

$$p = \frac{1}{L_1 C_1 L_2 C_2} \quad (2.3a)$$

$$s = -\frac{L_2 C_1 + L_1 C_1 + L_2 C_2}{L_1 C_1 L_2 C_2} \quad (2.3b)$$

It's easy to see that  $p > 0$  and  $s < 0$  because the components values are all strictly positive, so both  $t_1$  and  $t_2$  must be negative, that finally proves that the solutions are complex. Given that all the coefficients of the denominator of (2.1) are real, all its complex solutions will come in conjugate pairs, so the four poles will be complex conjugate.

### 2.3.2.3 AC response

We expect the amplitude bode plot to start with +40dB per decade, then two resonant peaks interspersed by a flat zone, and a rapid loss of gain of -40dB per decade in the high frequencies. The simulated plot follows: This graphic is obtained if  $L_1 = L_2 = 25\mu\text{H}$  and  $C_1 = C_2 = 100\text{nF}$ .

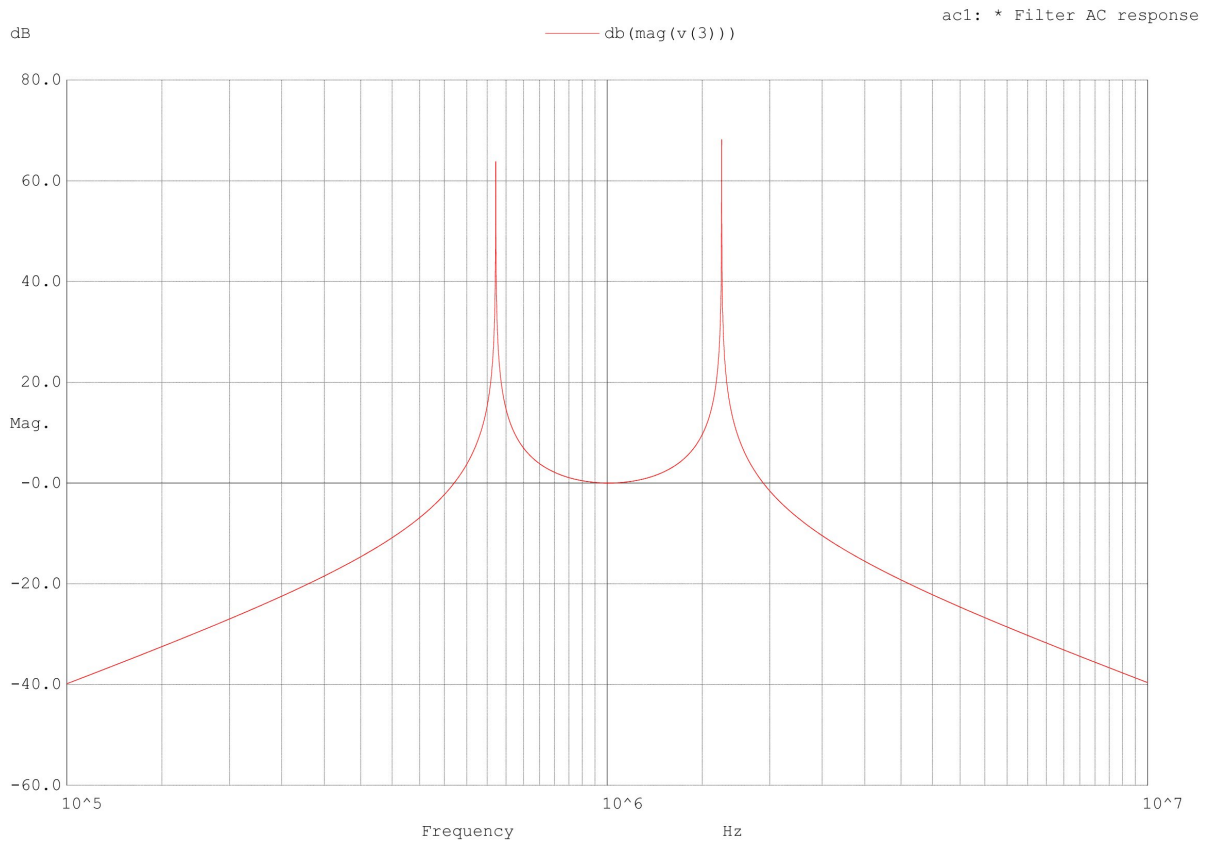


Figure 2.7: Filter AC response

### 2.3.2.4 Impedance

The magnet impedance between  $in_1$  and  $out_{24}$  is shown in figure 2.8.

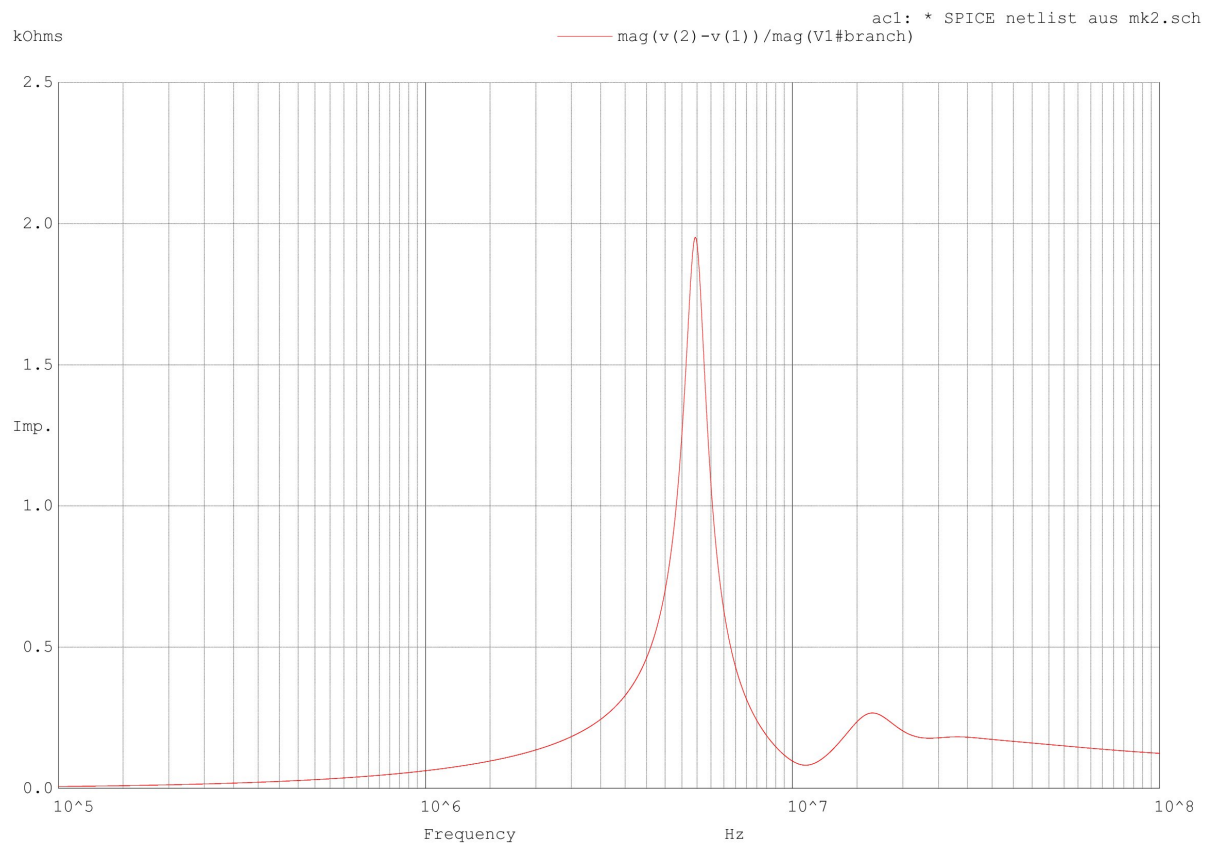


Figure 2.8: Magnet impedance

### 2.3.3 Modified filter

The first simulations showed that the filter as of figure 2.6 did not perform very well, mainly because of its pure reactive characteristics that didn't allow the simulator to perform well. Some parasitic resistors were then added and their respective values estimated in order to obtain valuable simulated data.

#### 2.3.3.1 Schematic

The following circuit presents various parasitic components and is somewhat more realistic than the only reactive one.

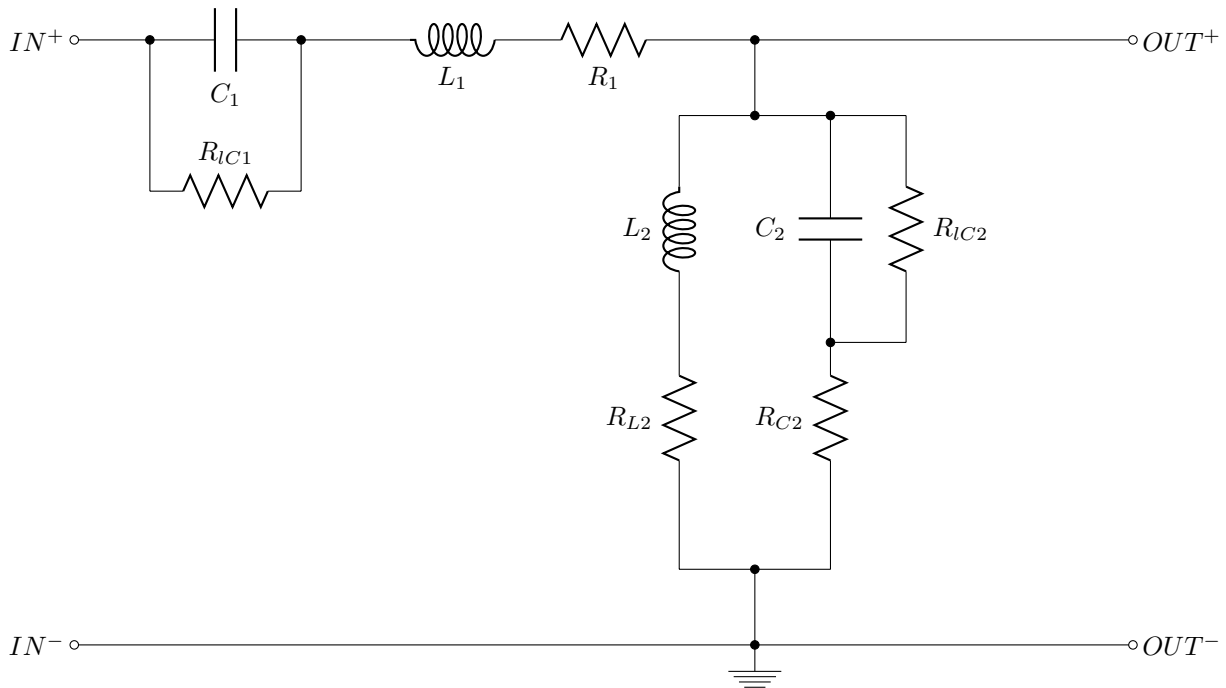


Figure 2.9: Realistic filter

Where:

- $R_{1C1}$  and  $R_{1C2}$  are the dielectric loss resistors
- $R_1$ ,  $R_{L2}$  and  $R_{C2}$  are the components lead resistors

The starting component values used for dimensioning follow.

- $R_{1C1} = R_{1C2} = 1\text{M}\Omega$
- $R_1 = R_{C2} = R_{L2} = 1\text{m}\Omega$
- $L_1 = 1\mu\text{H}$
- $C_1 = 1\text{nF}$
- $L_2 = 2\mu\text{H}$
- $C_2 = 100\text{nF}$

To couple the filter and the magnet a 1:1 transformer was used, both primary and secondary coil measuring  $10\mu\text{H}$ .

### 2.3.4 First prototype

A low power, low cost prototype was built using some scrap ferrite cores for the transformer and the tuning coils.

#### 2.3.4.1 Construction

The realization of the prototype was quite straightforward. The components were a few, and the only challenge was building the coils and the transformer. The tuning coils were built winding thick insulated wire around a rectangular shaped, linear ferrite core. The windings were made purposely loose to allow moving the core thus fine tuning the inductance value. The  $2\mu\text{H}$  inductance required four windings, while the  $1\mu\text{H}$  one required three.

The transformer was built winding the same thick wire on a linear ferrite core. To achieve the higher necessary inductance ten turns proved to be enough.

The whole circuit was air-mounted, but the connections were not made as short as possible to easily tune the coils and substitute components if necessary. Future prototypes might be built paying more attention to these details.



Figure 2.10: Filter prototype

Looking at figure 2.10 on the right and on the left one can respectively see the  $1\mu\text{H}$  and the  $2\mu\text{H}$

inductances, while the circuit sits on the transformer on the center. The square wave input is to be connected to the two top wires, while the magnet to the bottom two. Lastly, the orange capacitor is the 100nF one, while the brown capacitor is the 1nF smaller one.

### 2.3.4.2 Testing

The preliminary tests showed that the filter works as intended. Thanks to the tuning coils it is possible to regulate the phase and the amplitude of the high frequency harmonic, thus changing the magnet turnoff time.

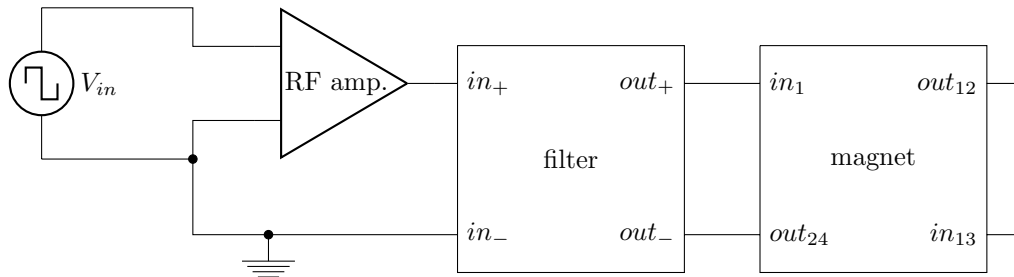


Figure 2.11: Testing setup

The square wave, coming from a signal generator, was fed directly to the RF amplifier that was then connected to the filter input. The magnet was finally connected to the filter output, and its two "back" inputs were short circuited. The power supplied by the amplifier was roughly 20W, and the peak-to-peak voltage measured differentially between  $in_1$  and  $out_{24}$  was 4 V.

Figure 2.12 shows the wave measured at the ends of the magnet. The measured frequency is about 296kHz and not 300kHz because the signal generator was tuned to match the filter and magnet resonant frequency. Figures 2.13a and 2.13b shows the enlargements of the wave crossing the zero, falling and rising respectively. The magnet seems off, i.e. the wave sits near zero, for about 100ns.

The oscilloscope data was saved so that precise off time could be calculated. The excel file used to do so is attached, and the threshold voltages can be changed to see the effects on the times. Setting the threshold at 5% of the peak-to-peak voltage, that is 200mV, produces 131.4ns and 131.6ns of turn off times for the falling and the rising fronts respectively.

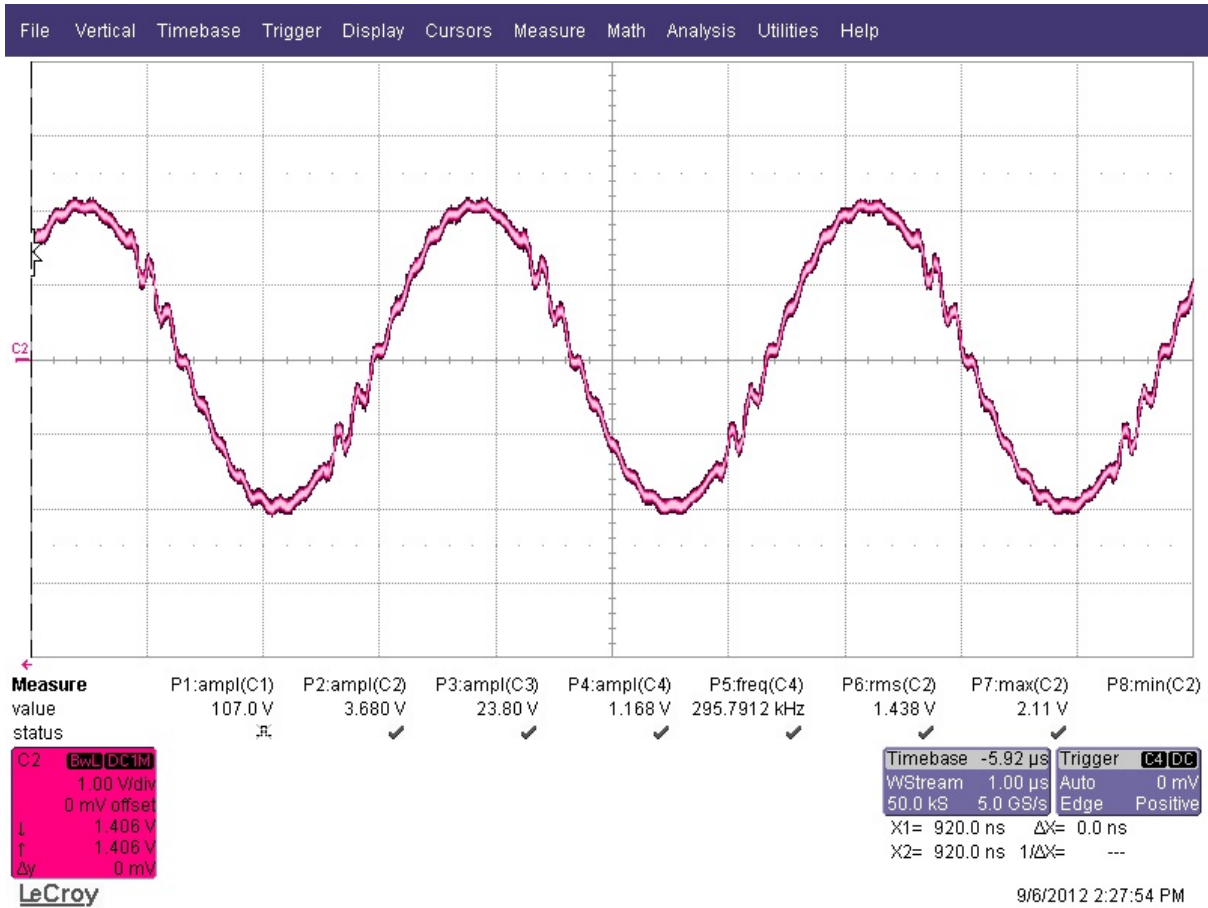


Figure 2.12: Measured voltage between  $in_1$  and  $out_{24}$

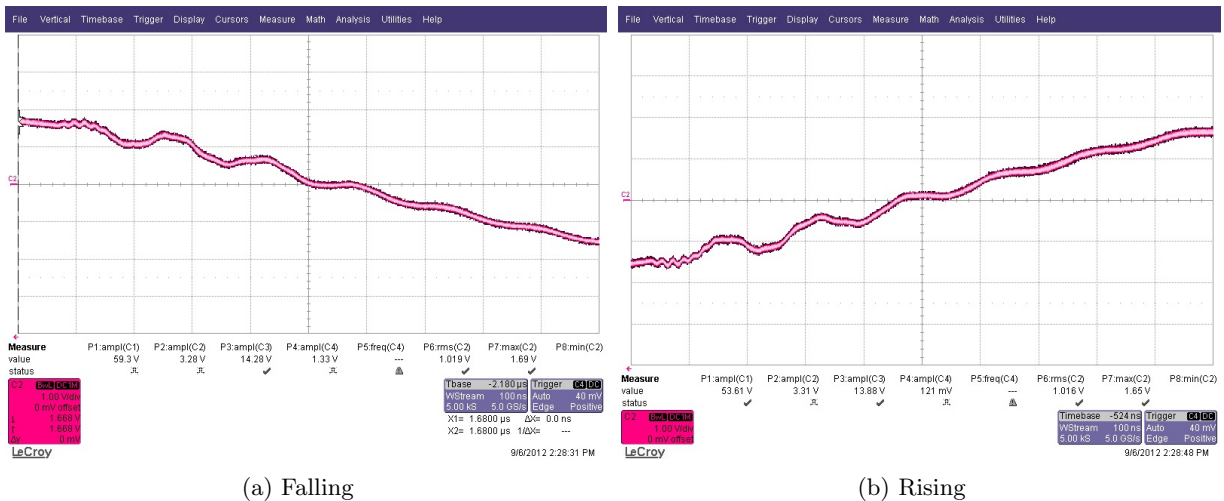


Figure 2.13: Output wave details

### **2.3.5 Further development**

The filter preliminary test was successful, but further investigations will be necessary to verify mainly its high power capabilities. Another prototype should be built, using more capacitors and bigger coils that can withstand the higher current and voltages, and the automated wave tuning controller feasibility should be discussed.

#### **2.3.5.1 Go for higher power**

Scale the filter up to the higher powers needed by one magnet should not be that tricky, mainly because it is all passive and ideally non resistive. The components lead resistances will probably become a problem, but at less than 2kW, that is the power we need, they should still be small enough.

If all the magnets needed will be excited by one filter the power demand will probably create many problems when building it, but other issues will show up, such as guaranteeing the phase between the various magnetic fields. The best solution will probably be to build one filter per magnet, or a few of them, together with its control circuit.

#### **2.3.5.2 Automated wave tuning**

Thanks to the filter tuning coils an automated digital wave tuning device can be built, although a deeper study is necessary. The magnetic field can be picked up with a small coil inside the magnet and then be fed through a zero crossing analog detector after proper amplification. The zero crossing circuit will provide the controller a clean digital signal that will toggle when the magnetic field modulus is below a settable value. The controller will then apply simple control algorithms and pilot the linear actuators connected to the coils ferrite cores to shape the wave as requested. All the controllers can be wired together to guarantee the relative phase between magnets or group of magnets, and communication to a computer or other devices can be implemented too.

It is even possible to measure the average field in the magnet and regulate the power fed to it in order to meet the specifications.

### **2.3.6 Conclusions**

Although the idea is at a preliminary stage, and only a few tests could be run, the results acquired seems very promising. The feasibility of the filter seems guaranteed by its intrinsic characteristics, even at higher powers, and an automated control can be implemented. It's still to be understood if such a circuit will be cost effective, given that all the complications it introduces will lead to higher costs, but less magnets will probably be necessary if the power will be sufficiently high.

# Chapter 3

## Ringer

### 3.1 Introduction

There are various methods to characterize and measure all the parameters of a coil, one of which is using a ringer. A ringer circuit basically consists of a capacitor, a charging circuit and a discharge switch. To measure the coil parameters you need to connect it to the discharge leads, collect the transient voltage and/or current response and finally calculate the parameters of interest.

### 3.2 Theoretical treatise and setup

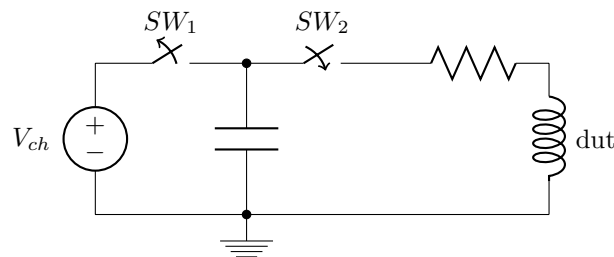


Figure 3.1: Measurement setup

Figure 3.1 represents a simplified scheme of a coil connected to a ringer. The series resistor represents the wire resistances, and the switches show the operating mode of the ringer. First the capacitor is charged through  $V_{ch}$ , then both switches toggles and the capacitor is discharged in the device under test. The resulting circuit is a series RLC circuit and is well treated in literature. The voltage across the coil can be captured, and according to theoretical treatise its form will be:

$$V_0 \cdot e^{-\alpha t} \cos(\omega_d t + \phi) \quad (3.1)$$

Where:

- $V_0$  is determined by initial conditions
- $\alpha$  is the attenuation
- $\omega_d$  is the dampened resonant frequency
- $\phi$  is the phase

Given that the phase can be conveniently chosen to be zero and  $V_0$  is not derived from theory but rather measured, the only two quantities that we are interested in are  $\alpha$  and  $\omega_d$ . The theory again tells us that:

$$\omega_0 = \frac{1}{\sqrt{LC}} = \sqrt{\omega_d^2 + \alpha^2} \quad (3.2a)$$

$$\alpha = \frac{R}{2L} \quad (3.2b)$$

From which we can easily get:

$$L = \frac{1}{C(\omega_d^2 + \alpha^2)} \quad (3.3a)$$

$$R = 2\alpha L \quad (3.3b)$$

Using 3.3a and 3.3b it is possible to calculate the coil inductance value and its series resistance, as long as the ringer capacitor capacitance value is accurately known.

### 3.3 Conclusions

Theoretical treatise showed that measuring some coil parameters using the ringer should be possible. Some questions about feasibility remain, though:

- Is it possible to measure  $\alpha$  and  $\omega_d$  from the oscilloscope plot without introducing big errors?
- Can the coil withstand high voltage, high current related stress?
- Is it possible to check the coil insulation by means of the ringer?

However this project showed many potentialities that deserve further investigation.